

**Identification of genetic markers of resistance to macrolide class antibiotics in *Mannheimia*
haemolytica isolates from a Saskatchewan feedlot**

Darien Deschner^a, Maarten J. Voordouw^a, Champika Fernando^a, John Campbell^b, Cheryl L.
Waldner^b, Janet E. Hill^{a#}

^a Department of Veterinary Microbiology, University of Saskatchewan, Saskatoon, Canada

^b Department of Large Animal Clinical Sciences, University of Saskatchewan, Saskatoon,
Canada

Running head: Markers of macrolide resistance in *Mannheimia haemolytica*

[#]Correspondence: Janet.Hill@usask.ca

Abstract

Mannheimia haemolytica is a major contributor to bovine respiratory disease (BRD), which causes substantial economic losses to the beef industry, and there is an urgent need for rapid and accurate diagnostic tests to provide evidence for treatment decisions and support antimicrobial stewardship. Diagnostic sequencing can provide information about antimicrobial resistance genes in *M. haemolytica* more rapidly than conventional diagnostics. Realizing the full potential of diagnostic sequencing requires a comprehensive understanding of the genetic markers of antimicrobial resistance. We identified genetic markers of resistance in *M. haemolytica* to macrolide class antibiotics commonly used for control of BRD. Genome sequences were determined for 99 *M. haemolytica* isolates with six different susceptibility phenotypes collected over two years from a feedlot in Saskatchewan, Canada. Known macrolide resistance genes *estT*, *msr*(E), and *mph*(E) were identified in most resistant isolates within predicted integrative and conjugative elements (ICEs). ICE sequences lacking antibiotic resistance genes were detected in 10/47 susceptible isolates. No resistance-associated polymorphisms were detected in ribosomal RNA genes, although previously unreported mutations in the L22 and L23 ribosomal proteins were identified in 12 and 27 resistant isolates, respectively. Pangenome analysis led to the identification of 79 genes associated with resistance to gamithromycin, of which 95% (75/79) had no functional annotation. Most of the observed phenotypic resistance was explained by previously identified antibiotic resistance genes, although resistance to the macrolides gamithromycin and tulathromycin was not explained in 39/47 isolates, demonstrating the need for continued surveillance for novel determinants of macrolide resistance.

Importance

Bovine respiratory disease is the costliest disease of beef cattle in North America, and the most common reason for injectable antibiotic use in beef cattle. Metagenomic sequencing offers the potential to make economically significant reductions in turnaround time for diagnostic information for evidence-based selection of antibiotics for use in the feedlot. The success of diagnostic sequencing depends on a comprehensive catalog of antimicrobial resistance genes and other genome features associated with reduced susceptibility. We analysed the genome sequences of isolates of *Mannheimia haemolytica*, a major bovine respiratory disease pathogen, and identified both previously known and novel genes associated with reduced susceptibility to macrolide class antimicrobials. These findings reinforce the need for ongoing surveillance for markers of antimicrobial resistance to support improved diagnostics and antimicrobial stewardship.

Introduction

Bovine respiratory disease (BRD) is a major concern in the feedlot industry where it is estimated to cause more than US\$3 billion in losses each year globally (1). BRD is commonly controlled by treating high-risk groups of animals with antibiotics on arrival at the feedlot in a practice known as metaphylaxis (2, 3), which has been associated with selection of antimicrobial resistant bacteria (reviewed in (4)). Concerns about antimicrobial resistance (AMR) resulted in the passage of legislation increasing oversight of antimicrobial use in animal agriculture in Canada and the European Union (5–8). To meet the challenge of reducing the use of antibiotics and using antibiotics more prudently, veterinarians and producers need rapid and accurate diagnostic tests and sampling strategies to provide the best evidence for treatment decisions.

Diagnostic sequencing is the application of sequencing technologies in medical and veterinary diagnostics (9). The biggest benefit of diagnostic sequencing over traditional methods is the speed at which it can provide an answer, taking hours to get a result where traditional methods often take days. In the specific case of detecting AMR, the reduced turnaround time is due to bypassing the requirement for time-consuming culture and antimicrobial susceptibility testing of bacteria in the laboratory. Identifying genetic markers of resistance allows veterinarians to make evidence-based decisions about appropriate antibiotics, while avoiding prescribing ineffective antibiotics. Realizing the potential of diagnostic sequencing requires a comprehensive and informative database of all genetic markers of resistance (genes and mutations) in pathogens of interest.

Mannheimia haemolytica is the major bacterial agent associated with BRD in North America (10) and macrolide class antibiotics are often the choice for use in metaphylaxis or as

first-line therapeutics, which has resulted in the evolution of increased resistance to these drugs (11–13). A number of macrolide resistance genes and mutations have been identified in *M. haemolytica*, however, the recent characterization of a macrolide esterase encoded on a plasmid carried by a *Sphingobacterium faecium* isolate recovered from a feedlot water trough, and widely distributed among animal pathogens including *M. haemolytica*, highlights the need for further studies to expand our knowledge of the genetic markers of macrolide resistance in cattle-associated bacteria (14–16). Antimicrobial resistance genes (ARGs) in *M. haemolytica* are frequently carried within mobile genetic elements known as integrative and conjugative elements (ICEs) that are capable of spreading ARGs to related species such as *Pasteurella multocida* (17, 18). In addition to ARGs, single nucleotide polymorphisms (SNPs) in the genes encoding the cellular targets of macrolides (ribosomal RNAs and ribosomal proteins) have also been known to confer macrolide resistance in *M. haemolytica* and other species (19).

In the current study, we analysed the whole genome sequences of macrolide resistant and susceptible *M. haemolytica* isolates collected over two years from a feedlot in Saskatchewan, Canada, to identify the genetic markers of macrolide resistance. Our objective was to identify known AMR genes and mutations, and to identify potentially novel markers associated with macrolide resistance with the goal of enhancing *M. haemolytica* databases used in diagnostic sequencing.

Materials & Methods

Selection of *M. haemolytica* isolates

Study isolates were selected from an existing collection of *M. haemolytica* isolates (20). The collection was derived from deep nasopharyngeal swabs collected from 800 cattle at the

Livestock and Forage Centre of Excellence (LFCE) in the fall of 2020 and in the fall of 2021 at three time points: on arrival, 13 days after arrival, and 36 days after arrival. Animals were recently weaned steers of various beef breeds sourced from a local auction market and originating from a combined total of 292 unique farming operations (20). Samples were cultured to select for *M. haemolytica*, identification was confirmed by matrix-assisted laser desorption/ionization time-of-flight mass spectrometry (MALDI-TOF MS; Bruker Daltonics, Billerica, MA), and susceptibility of one *M. haemolytica* isolate per animal was determined using the Sensititre system (Bovine/Porcine BOPO7F Vet AST Plate) at Prairie Diagnostic Services (PDS, Saskatoon). Isolates were classified as either resistant, intermediate, or susceptible in accordance with the breakpoints established by the Clinical Laboratory Standards Institute (Table S1, (21)). Isolates classified as intermediate were categorized as resistant (non-wild type) in all subsequent analyses.

We selected 52 macrolide resistant and 47 susceptible isolates for further study. Fifteen isolates were selected in the fall 2020 collection period with one collected on arrival and the remaining fourteen at 13 days post-arrival. Eighty-four isolates were selected in the fall 2021 collection period with three collected on arrival, 49 at 13 days post-arrival, and 21 at 36 days post-arrival, two from sick animals, one from a dead animal, and eight from a collection of isolates selectively cultured on 5% sheep blood agar plates supplemented with 16 µg/mL of tulathromycin. Six of the selectively cultured isolates were derived from samples collected 36 days post-arrival, one from a sick animal and one from a dead animal. Antimicrobial susceptibility testing of the selectively cultured isolates was performed as described above. To maximize diversity, each of the selected isolates was from an animal sourced from a different farm of origin and whenever possible we selected a susceptible isolate from the same time point

and pen for each resistant isolate. The 52 selected resistant isolates had a variety of phenotypes, although all were resistant to at least one of the four tested macrolides: gamithromycin (GAM), tulathromycin (TULA), tildipirosin (TILD), and tilmicosin (TILM). Many of the isolates were also resistant to tetracycline (TET). We included the results for tetracycline resistance in our analysis due to its common use in feedlots for the treatment and prevention of BRD and the strong association of tetracycline resistance genes with ICEs (11).

Genomic DNA Extraction

Isolates were cultured aerobically on 5% sheep blood agar plates at 37°C for 24 hr, and one colony was selected and grown aerobically in 7 mL of brain heart infusion (BHI) broth at 37°C for 24 hr with shaking at 200 rpm. Two 3 mL aliquots of each broth culture were pelleted, and genomic DNA was then extracted using a salting-out protocol as previously described (22). DNA concentration of extracts was determined using spectrophotometry (Nanodrop 2000) and electrophoresis in 0.8% agarose was used to assess fragmentation and to detect RNA contamination. Extracts that were found to have visible RNA contamination were then incubated with 5 µL of RNase A (100 mg/mL) at 37°C for 1 hour, followed by the sodium acetate and ethanol precipitation steps of the salting-out protocol.

To confirm the identity of the genomic DNA as *M. haemolytica*, cpn60 PCR and amplicon sequencing were performed using either universal cpn60 PCR primers (23) or *M. haemolytica* specific cpn60 primers (Forward: GCG ATT GTA AAC GAG GGC TT; Reverse: TGA CCG ACT GTT GAA TCT GAG). Sequencing was performed by the Sanger method and the forward and reverse primer reads were combined using the pregap4 and gap4 software to produce a consensus sequence that was aligned to the cpnDB database (24) using the FASTA-

based sequence comparison tool. Sequence identity of at least 90% over the length of the amplicon sequence was the minimum threshold for identification as *M. haemolytica*.

As a final quality check, all extracts were assessed for DNA concentration immediately prior to Illumina library preparation using fluorometry (Qubit dsDNA Broad Range Assay Kit, Invitrogen). A minimum DNA concentration of 20 ng/μL was required for an extract to be included in Illumina library preparation.

Whole Genome Sequencing

Illumina sequencing libraries were prepared using the Nextera XT Library Prep Kit (Illumina) according to the manufacturer's instructions. Libraries were first diluted to a DNA concentration of 0.2 ng/μL. Following indexing and purification, fragment size distribution in prepared libraries was assessed (Bioanalyzer 2100, Agilent) and quantified using the Qubit ds Broad Range assay kit (Invitrogen). Libraries were manually normalized to a concentration of 4 nM and then pooled and diluted to 8 pM with a final concentration of 1% PhiX DNA and sequenced using the 500 cycle MiSeq Reagent Kit v2 (2 x 250 bp) on the Illumina MiSeq platform. Up to 24 genomes were sequenced per flow cell.

Isolates were also sequenced on a GridION platform using the ligation sequencing kit (SQK-LSK109) and the FLO-MIN106 flow cell (PDS, Saskatoon). MinKnow v 22.03.2 was the operating system and Guppy v 6.06 was used for base calling. A Qscore cut-off threshold of 9 was utilized for all reads, with those below the cut-off being excluded from the sequencing output.

Whole Genome Sequence Assembly

Raw, demultiplexed, Illumina reads were processed using Trimmomatic with a sliding window of 4, quality score threshold of 20 and minimum sequence length of 36 bp (25). Raw nanopore reads were processed using Filtlong v 0.2.1 with a minimum length of 1,000 bp. Quality-filtered reads from both Illumina and Nanopore sequencing were utilized for hybrid *de novo* whole genome assembly using Unicycler v 0.5.0 with the default settings (26). Whole genome sequences were then assessed for quality using seqkit v 2.3.0 (27) and annotated using Prokka v 1.14.5 (28).

Identification of Antibiotic Resistance Genes

Whole genome assemblies were screened for known antibiotic resistance genes and mutations using the Resistance Gene Identifier (RGI) algorithm provided by the Comprehensive Antibiotic Resistance Database (CARD) using the default settings and database v 3.2.5 (29, 30).

The macrolide esterase *estT* was not present in the utilized version of the database, and an alternative approach was therefore taken to examine the whole genome assemblies for the presence of this gene. In Geneious Prime v 2023.2.1, a BLAST database was constructed consisting of the whole genome assemblies of the study isolates. The reference sequence for *estT* was then downloaded from the reference sequence for *Sphingobacterium faecium* strain WB1 plasmid pWB1 (CP094932.1) and compared against this database using the Geneious built-in BLAST software to identify homologous regions of the genome assemblies.

Identification of 23S rRNA, L4 and L22 mutations

Barrnap v 0.9 (31) was used to extract all copies of 23S rRNA gene sequences from *M. haemolytica* genome assemblies and then 23S rRNA gene sequences were aligned using snippy v

4.6.0 (32) to the reference sequence from *M. haemolytica* USDA-ARS-USMARC-183 (Genbank Accession NR_103087) with nucleotide numbering according to this sequence.

For the L4 and L22 ribosomal proteins, two custom shell scripts were utilized that extracted the L4 and 22 ribosomal protein amino acid sequences from the Prokka annotations (Supplemental File 1). The ribosomal protein amino acid sequences were then aligned to the reference sequences from *M. haemolytica* strain USMARC_2286 (L4: AGR7646 and L22: AGR73803) using BLASTp and any amino acid differences were recorded manually.

Pangenome Analysis

All whole genome sequences were submitted to Roary analysis software (v 1.7.7) alongside a reference strain for the two *M. haemolytica* genotypes 1 and 2 (genotype 1= CP017518; genotype 2= CP017519) (33). Gene clusters were sorted into one of four categories: core, soft-core, cloud and shell, based on how many of the isolates in the examined dataset the gene cluster appeared in. With a total input of 101 genomes (2 references and 99 study isolates), core genes were those found in 99-101 isolates, soft core in 95-98 isolates, shell in 15-94 isolates and cloud in less than 15 isolates. A multiFASTA alignment of core genes was produced using MAFFT using the -e and -n flags. The roary_plots.py python script was then utilized to generate three outputs: a pangenome matrix, a frequency plot, and a pie chart. A phylogenetic tree was additionally generated using the core gene multiFASTA alignment as the input for FastTree (34). The genotype of each isolate was inferred based on proximity to the genotype 1 and 2 reference sequences in the phylogenetic tree.

Whole Genome SNP Analysis

To reduce the impact of assembly errors in the identification of SNPs, all whole genome sequences were polished using Pilon v 1.24 (35). Each genome underwent a minimum of five rounds of pilon polishing prior to whole genome SNP analysis following the method described in (36). In brief, genomes were indexed using Hisat2 v 2.2.1 (37) to produce a SAM file, which was converted to a BAM file, and then sorted and indexed using Samtools v 1.17 (38) with the resulting BAM file being used as input to Pilon.

For whole genome SNP analysis, we utilized the snippy-multi function of snippy v 4.6.0 to generate a .VCF file for each analyzed genome containing all the identified SNPs (32). To reduce the number of SNPs that were related to genotype, we chose to analyze the two genotypes of *M. haemolytica* separately and used a susceptible isolate of either genotype as the reference genome (37787 S-06 for genotype 1 and 34455 S-12 for genotype 2). Finally, pyseer v 1.3.10 was used to identify SNPs that were associated with phenotypic resistance to macrolide class antibiotics for each of the individual genotypes using a p-value cut-off of 0.05, a maximum allele frequency equivalent to the proportion of phenotypically resistant isolates included in the analysis (0.5 for genotype 1 and for 0.54 for genotype 2), and the elastic net whole genome model (39, 40). The odds ratio of each SNP was then determined using Microsoft Excel for Microsoft 365 MSO (Version 2308 Build 16.016731.20052) 64-bit. SNPs that possessed an odds ratio lower than 0.8 or greater than 1.2 were considered as potentially explanatory for the observed phenotype.

Association of Phenotypic Macrolide Resistance with Known AMR Genes and Candidate Genes

Generalized linear models (GLMs) with binomial errors were used to confirm the associations between known AMR genes and phenotypic resistance to each of the five antimicrobial drugs (GAM, TULA, TILD, TILM, TET) using the `glm()` function in R (41). Resistance to each of the five drugs was coded as a binomial variable as susceptible (0) or resistant (1). The known AMR genes *tet(H)*, *estT*, APH(3')-1a, APH(3'')-1b, and APH(6)-1d were present in the same 44 isolates. Similarly, the known AMR genes *msr(E)* and *mph(E)* were present in the same eight isolates. As statistical analyses cannot include identical explanatory factors, only *tet(H)* and *msr(E)* were included in the GLMs (i.e., the other 5 genes were not included in the analysis because they were redundant with *tet(H)* and *msr(E)*). Genotype was also included as an explanatory factor as it had previously been shown to be associated with phenotypic resistance (42). For these GLMs, a p-value ≤ 0.05 was significant.

The same GLM approach was used to test the association between phenotypic resistance and the candidate genes that were identified in the pangenome analysis. The sign of the slope relating AMR to the presence/absence of a gene indicates whether the gene confers resistance (positive slope) or susceptibility (negative slope) to a given drug. For these GLMs, a Bonferroni-corrected p-value was used where 0.05 was divided by the number of candidate genes. Both unifactorial and multifactorial GLMs were performed. The unifactorial GLMs only included the candidate gene of interest, whereas the multifactorial GLMs also included genotype, *tet(H)*, and *msr(E)*.

Protein structure predictions and alignments

Amino acid sequences were aligned with MUSCLE in Geneious Prime using default settings. Secondary structures were predicted with PSIPRED and DISOPRED3, and protein structure prediction from primary amino acid sequences was performed with DMPFold within the PSIPRED Protein Analysis Workbench (43). Structure visualization and alignments were generated with Pymol (Schrodinger, Inc.).

Mobile Genetic Element Analysis

All 99 genome sequences of the study isolates were submitted to the online web tool implementation of ICEfinder for identification of putative ICEs (44). The sequences of identified putative ICEs and integrative and mobilizable elements (IMEs) were downloaded and information such as the insertion site and direct repeat sequence were recorded in an Excel spreadsheet. Putative ICE sequences that were found to possess ≤ 10 type 4 secretion system (T4SS) components and/or lacked an identified insertion site were removed from further analysis. Manual curation and comparisons of the putative ICE sequences were done in Geneious Prime. To determine if the identified putative ICE sequences were novel or homologues of the previously identified ICE*Mhl* (45), the representative consensus sequence for each ICE was aligned to ICE*Mhl* from *M. haemolytica* 42548 using BLASTn (ICEberg database ID ICEO_0000728) (46).

Results & Discussion

Description of Isolates

Study isolates were initially characterized by their antimicrobial resistance phenotype resulting in six groups (Table 1, Table S2).

Genome sequencing and assembly

The average length of the assembled genomes ($n = 99$) was 2.9 Mb (range 2.5 Mb – 5.2 Mb) with an average N50 score of 2.6 Mb (range 0.6 Mb – 2.7 Mb). The median number of contigs per assembly was 2 (range 1 – 26). The average estimated coverage for assemblies was $158\times$ (median $131\times$, range $23\times$ – $578\times$). Isolate 38241 S-35 was not included in the whole genome SNP analysis due to insufficient coverage with high quality Illumina reads. Based on phylogenetic analysis of core genomes identified in the pangenome analysis described below, most isolates (82/99) were identified as genotype 2, and the remainder (17/99) as genotype 1 (Figure S1). A detailed summary of the characteristics of the genome assemblies is provided in Table S3.

Antibiotic Resistance Gene Identification

Antibiotic resistance genes were identified in each whole genome sequence utilizing the RGI software provided by CARD, where “perfect” hits were considered to represent the presence of a given gene, and “strict” hits were considered to represent the presence of a gene providing the resulting hit had a percent identity of at least 90% and a percent length between 99-101%, as calculated by dividing the length of the query protein by the length of the reference protein (Table 2). This analysis revealed two distinct genetic profiles that together accounted for 94% (49/52) of the phenotypically macrolide resistant isolates. One genetic profile consisted of the known macrolide resistance genes *msr*(E) and *mph*(E), which encode a ribosomal protection protein and a macrolide inactivating phosphotransferase, respectively (47, 48), and the sulfonamide resistance gene *sul2*. The other genetic profile included the tetracycline resistance gene *tet*(H) and its regulator *tetR*, the aminoglycoside resistance genes APH(3’)-1b, APH(3’)-1a, and APH(6)-1d, and *sul2*.

Resistance genes *msr*(E) and *mph*(E) were identified in only 8/52 isolates, all of which had the GAM/TULA resistance phenotype (Table 2). Monomethyltransferase encoding gene *erm42*, previously associated with macrolide resistance (16), was not detected in any isolate. In all the remaining macrolide resistant isolates, the *tet*(H) gene was detected alongside the three aminoglycoside resistance genes APH(3'')-1b, APH(3')-1a, and APH(6)-1d (Table 2). The presence of *tet*(H) has been strongly associated with the presence of ICEs, and the identified aminoglycoside resistance genes have frequently been identified on ICE*Mhl* (17, 18, 49, 50). The sulfonamide resistance gene *sul2* was identified in all but three phenotypically macrolide resistant isolates, which may reflect *sul2* having been incidentally selected for alongside macrolide resistance as part of the same mobile element. Regardless of the origin of the *sul2* gene, CLSI presently lacks a breakpoint for sulfadimethoxine for *M. haemolytica* so no determination on the resistance profile of the isolates was made. No known antibiotic resistance genes were identified in the phenotypically macrolide susceptible isolates (Table 2).

Macrolide esterase gene *estT* was detected in all resistant isolates except for those with the GAM/TULA resistance phenotype. *estT* was consistently annotated by Prokka as *rdmC*, a methylesterase involved in the biosynthesis of the anthracycline antibiotic aclacinomycin (51). The identification of *estT* offers a partial explanation for the observed phenotypic resistance, however, it has been demonstrated biochemically that the enzyme encoded by *estT* has no activity on gamithromycin (GAM) or tulathromycin (TULA) (14). Thus, its presence fails to explain the observed resistance to these drugs in the GAM/TULA/TET/TILM/TILD, TULA/TET/TILM/TILD, and GAM/TULA/TILM isolates. We used GLMs with binomial errors to test whether genotype, *tet*(H) (identical presence/absence pattern to *estT*), and *msr*(E) (identical presence/absence pattern to *mph*(E)) were associated with phenotypic resistance to

each of the five individual antimicrobial drugs (Table 3). The unifactorial GLM found that genotype was significantly associated with resistance to TET, TILD, and TILM, and that *tet(H)* and *msr(E)* were significantly associated with phenotypic resistance to all five tested antimicrobials. The results changed when all three explanatory factors were included in the multi-factorial GLM; *tet(H)* was significantly associated with phenotypic resistance to all five tested antimicrobials, and *msr(E)* was significantly associated with phenotypic resistance to GAM and TULA, consistent with the observations in Table 2. The association of *tet(H)* with macrolide resistance is almost certainly due to the strong linkage of *tet(H)* with ICEs and not due to any role of the *tet(H)* gene product in reduced susceptibility to macrolides. In the multifactorial GLM, genotype was not associated with phenotypic resistance to any antimicrobial drugs. The association between genotype and resistance to TET, TILM, and TILD in the unifactorial GLM was probably driven by differences in the prevalence of *tet(H)* in genotypes 1 and 2 (0.0% (0/17) and 52% (44/84), respectively). The lack of a relationship between genotype and resistance to any of the antibiotics tested somewhat contradicts previous reports that genotype 2 isolates are more likely to carry known antibiotic resistance genes (42), however, the limited number of genotype 1 isolates included in this study means this lack of association should be interpreted with caution.

23S rRNA, L4 and L22 polymorphism identification

Mutations in the cellular targets of macrolides, 23S rRNA and ribosomal proteins L4 and L22, have previously been associated with reduced susceptibility (47, 52). Six copies of the 23S rRNA gene were identified in each of the study isolates and no resistance associated polymorphisms were identified relative to a reference sequence (NR_103087) (Table S3). No resistance associated differences were identified in the amino acid sequences of the L4 ribosomal

protein, however, in the L22 ribosomal protein, a D94A amino acid difference occurred in 23% (12/52) of the macrolide resistant isolates and none of the susceptible isolates (Table S3). Of the twelve isolates with the D94A L22 variant, all were genotype 2, and seven isolates had the TULA/TET/TILM/TILD resistance phenotype, three isolates had the TET/TILM/TILD phenotype, and two isolates had the GAM/TULA/TET/TILM/TILD phenotype.

Among the 12 isolates with the L22 ribosomal protein D94A sequence variant, the only commonality was phenotypic resistance to the 16-membered lactone ring macrolides TILM and TILD, which suggests this variant may alter the binding affinity of 16-membered lactone ring macrolides but not the binding affinity of gamithromycin (GAM, a 15-membered lactone ring macrolide) or tulathromycin (TULA, a triamilide macrolide comprising a 90:10 mixture of 15-membered lactone ring and 13-membered lactone ring regioisomers (53)).

Whole Genome SNP Analysis

To identify potentially novel sequence variants associated with reduced macrolide susceptibility, we conducted a genome-wide SNP analysis of genotype 1 and genotype 2 isolates. A total of 325 sequence variants (SNPs, insertions, or deletions) were initially identified as having a significant association ($p \leq 0.05$) with observed phenotypic macrolide resistance (any of the phenotypes in Table 1) in the genotype 1 isolates, however, all odds ratios were between 0.8 – 1.2. For the examined genotype 2 isolates, a total of 1,031 sequence variants were identified, with all odds ratios falling between 0.8 – 1.2. These results suggest that SNPs are not an explanation for the observed phenotypic macrolide resistance (Tables S4 and S5).

Pangenome Analysis

A total of 101 isolates were included in the pangenome analysis, 99 study isolates and two reference strains representing genotype 1 and genotype 2. A total of 8,325 gene clusters were identified in the pangenome with each isolate possessing an average of 2,765 (median = 2,766) gene clusters (range = 2,486 – 5,181) (Table S6). Of the 8,325 gene clusters identified, 1,651 were identified as core genes (i.e., were present in 99-101 of the 101 examined isolates), which were used in a phylogenetic analysis to identify isolates as genotype 1 (17 isolates) or genotype 2 (82 isolates) based on their distance to and from the two reference genomes (Figure S1).

To discover novel AMR genes, we used the same GLM approach for each of the five macrolide antimicrobials, as described previously. The unifactorial GLM only included the candidate gene of interest as the single explanatory factor. The multifactorial GLM included the candidate gene of interest, but also genotype, *tet*(H) and *msr*(E) as explanatory factors. Of the 8,135 genes identified in the pangenome, 1,413 were part of the core genome (i.e., they were present in all isolates), and these genes were not analysed for their association with AMR. Of the remaining 6,912 genes, 24 genes were excluded because they had the same presence/absence profile as *tet*(H), *msr*(E), or genotype, so that 6,888 candidate genes remained for GLM analysis (Table S7). A Bonferroni-corrected p-value of $0.05/6,888 = 7.26 \times 10^{-6}$ was used to determine whether a given candidate gene was significantly associated with phenotypic resistance to each of the five macrolide antimicrobials.

The unifactorial GLMs found 1,223 candidate genes that were significantly associated with phenotypic resistance to one or more of the tested macrolides (Table S8). In comparison, the multifactorial GLMs found only 150 candidate genes that were significantly associated with

resistance to GAM and no candidate genes that were significantly associated with resistance to any of the other four examined macrolide antimicrobials (Table S9). Thus, most of the genes in the unifactorial GLM were significant only because they were associated with either *tet*(H) and/or *msr*(E) in the genome of *M. haemolytica*. Below we further investigate the 150 genes identified in the multifactorial GLMs.

Of the 150 GAM-resistance associated genes, 79 were classified as putative resistance genes (GLM slope was positive) and 71 as putative susceptibility genes (GLM slope was negative). Of the 71 putative susceptibility genes, five had functional annotations: *clpP_2* (protease subunit), *mutS* (DNA mismatch repair protein), *rplW* (ribosomal protein L23), *ssb_4* (single-stranded DNA binding protein), and *tldD* (metalloprotease) (54–58), and the remainder were annotated as hypothetical/putative proteins.

Of the 79 putative resistance genes, four had functional annotations: *glpX_1* (fructose-1,6-bisphosphatase), *mnme* (tRNA modification GTPase), *rusA* (endonuclease that corrects defects during genetic recombination and some DNA repair), *ybcO* (putative nuclease) and the remainder were annotated as hypothetical/putative proteins (59–63). One possible connection to macrolide resistance is that the *mnme*-encoded GTPase may introduce a tRNA modification that prevents inhibition of protein translation by macrolide class antibiotics, however, as the motifs that macrolide class antibiotics recognize are in mRNA, this seems unlikely (64). Similarly, it is possible that the DNA repair activity of the *rusA*-encoded endonuclease may result in sequence changes that alter or eliminate macrolide activating motifs (64).

Further examination of the candidate genes identified in the GLM analysis revealed that the genes *mnme*, *mutS*, *tldD*, *rplW* and *glpX_1* had a variant with the inverse association (i.e.,

397 associated with susceptibility). These variants were identified as distinct genes rather than
398 variants due to the nature of the pangenome tool used (Roary). In identifying genes shared across
399 multiple genomes, an all-vs-all comparison of all coding sequences is conducted and based on a
400 defined threshold for “same”, coding sequences are grouped into genes and their distribution
401 among genomes is reported in the gene presence-absence table output from Roary. If multiple
402 variants of a gene are sufficiently different from each other so that they exceed the threshold for
403 clustering, they will be assigned to different gene groups. In this case, group_753 is a variant of
404 *mnmE*, group_508 for *mutS*, group_2294 for *tldD*, group_4230 for *rplW*, and group_452 for
405 *glpX_1*. Of particular interest is the *rplW* gene which encodes the L23 ribosomal protein, a
406 protein that is in close proximity to the nascent polypeptide exit tunnel of the ribosomal complex
407 (57). As mutations in other ribosomal proteins that surround the exit tunnel (L4 and L22) are
408 known to confer macrolide resistance, we further investigated the amino acid sequences of both
409 *rplW* variants and determined that the group_4230 variant has a 14 amino acid insertion relative
410 to the *rplW* sequence identified in susceptible isolates (Figure 1A). To determine the location of
411 the insertion within the three-dimensional structure of the protein, we aligned the *M. haemolytica*
412 *rplW* and group_4230 sequences with the L23 sequence of *Thermus thermophilus*, for which a
413 structure has been determined (65). The protein consists of a well-ordered part containing anti-
414 parallel beta-strands and a large loop that forms part of the peptide exit tunnel wall (65). The
415 predicted structure of the susceptibility-associated *rplW*-encoded L23 aligns well with *T.*
416 *thermophilus* L23 but the insertion in the group_4230 variant nearly doubles the size of the loop
417 (Figure 1B). This group_4230 variant of L23 was only identified in the 27 isolates with the
418 GAM/TULA/TET/TILM/TILD resistance phenotype, suggesting that alterations in the structure

of the peptide exit tunnel may contribute to the observed resistance to gamithromycin and/or tulathromycin in these isolates.

Mobile Genetic Element Analysis

ICEfinder initially identified 169 putative ICEs among the examined genome sequences (Table S10). After filtering the ICEfinder results as described in the methods, a total of 68 putative ICE sequences were identified across 66/99 (66%) of the isolates. At least one putative ICE sequence was identified in 19/47 (40%) of the susceptible isolates and 47/52 (90%) of the phenotypically resistant isolates. Manual examination of these sequences allowed us to consolidate them into three putative ICEs (ICEM*hI*-like01, ICE*Mh*GAMTULA, and ICE*Mh*Susceptible) based on shared direct repeat sequences, and number and types of cargo genes. For 37 of the putative ICEs, ICEfinder found an insertion site in a ribose-phosphate pyrophosphokinase gene, however, manual inspection of the flanking regions of this gene showed that these ICEs were in proximity to a tRNA-Leu gene, which is the typical insertion site for ICEs in *M. haemolytica* (18, 66, 67). On this basis, the ICE sequence was extended for all 37 of these putative ICEs to include the section between the boundaries initially identified by ICEfinder and the adjacent tRNA-Leu.

The sequences of all putative ICEs categorized as ICE*MhI*-like01 were extracted and a multiple sequence alignment of these sequences was performed to generate a consensus sequence. This process was repeated for ICE*Mh*GAMTULA and ICE*Mh*Susceptible (Figure 2), and the distribution of the ICEs among the study isolates was assessed (Table 4). The failure to identify any putative ICEs in seven of the resistant isolates may be attributable to lower assembly

quality for these isolates as all the genome sequences for these isolates consisted of six or more contigs.

ICEM*hI*-like01 was identified in 40/52 of the macrolide resistant isolates (Table 4). This ICE carried the known ARGs including APH(3')-1a, APH(3'')-1b, APH(6)-1, *estT*, *sul2*, *tet(H)*, and a gene encoding the *tet(H)* regulator TetR, as well as the copper resistance gene *mco*. ICEM*hI*-like01 was nearly identical in gene arrangement and sequence of the ARGs to the previously identified *M. haemolytica* ICEM*hI* in the region containing the ARGs. The portion of ICEM*hI*-like01 that failed to match to ICEM*hI* lacked any of the known ARGs, however this region did include genes encoding a MobH relaxase, an integrase and two transposases, which explains why this region was identified by ICEfinder as being part of a putative ICE (Figure 2, Figure S2).

ICEM*h*GAMTULA was found in 7/8 of the isolates resistant to gamithromycin and tulathromycin and was found to carry the known macrolide ARGs *msr(E)* and *mph(E)* alongside the sulfonamide resistance gene *sul2*. The *msr(E)* and *mph(E)* genes have previously been identified in ICEM*hI*-like ICEs, however, this has always been alongside other ARGs such as *tet(H)* (17, 18, 67). Further, ICEM*h*GAMTULA was found to share relatively little sequence similarity or synteny with ICEM*hI*, except for a region containing genes encoding a MobH relaxase, an integrase, and several ICE-associated genes (Figure 2). The similarity of ICEM*h*GAMTULA to ICEM*hI* in this region suggests that ICEM*h*GAMTULA is related to ICEM*hI* but has since lost other genes carried by ICEM*hI*. It is also possible that ICEM*h*GAMTULA is not an ICE but rather an integrated bacteriophage or an integrative and mobilizable element (IME) (44, 68), a suggestion supported by the limited number of T4SS

components it carries compared to *ICEMhI* (9 vs 14), which potentially inhibits the ability of *ICEMhGAMTULA* to undergo autonomous conjugative transfer.

ICEMhSusceptible does not carry any known ARGs but does contain genes encoding a MobH relaxase and an integrase, and some ICE-associated genes that are similar to the corresponding genes in *ICEMhI* in both arrangement and sequence identity (Figure 2). *ICEMhSusceptible* also included the same direct repeat sequence as *ICEMhI*-like01 and the insertion site of tRNA-Leucine. Due to the similarity in the “core” ICE genes to *ICEMhI* and the complete absence of ARGs, it is possible that *ICEMhSusceptible* represents a degraded version of *ICEMhI*, a bacteriophage or an IME. This suggestion is supported by the observation that *ICEMhGAMTULA* contained only nine type four secretion system (T4SS) components compared to the 14 T4SS components of *ICEMhI*, which would potentially limit its ability to undergo autonomous conjugative transfer.

Having established that the known macrolide ARGs *msr*(E), *mph*(E) and *estT*, and the known tetracycline resistance gene *tet*(H) were all present within an ICE, we next investigated whether any of the resistance-associated candidate genes identified in the multifactorial GLM analysis of the pangenome were also within the boundaries of predicted ICEs. A representative of each ICE was selected (*ICEMhI*-like01 from isolate MH077, *ICEMhGAMTULA* from isolate MH017, and *ICEMhSusceptible* from isolate 36267_S_17) and then inspected to determine whether any of the candidate genes associated with phenotypic resistance (as shown by the multifactorial GLM analysis) were located within the ICE sequence. None of the 150 candidate genes associated with resistance/susceptibility to GAM were identified within the boundaries of any of the putative ICEs. The lack of any putative susceptibility/resistance genes within ICEs

may be due to the inclusion of *tet(H)* as an explanatory factor in the multifactorial GLMs, as *tet(H)* is known to be strongly associated with the presence of ICE in *M. haemolytica*. Thus, including *tet(H)* in our multifactorial GLM would mean that any other genes also associated with the presence of an ICE would fail to be identified. Since macrolide class antimicrobials function by inhibiting translation (64), it is unlikely that the presence of any given gene would confer susceptibility to them and we therefore suggest that future investigations focus on the 79 putative GAM resistance genes identified using our multifactorial GLM analysis.

The identification of an ICE in susceptible isolates suggests that ICEs are widespread in *M. haemolytica* and that ICEs may confer some beneficial trait to their bacterial hosts other than AMR as, in most cases, ICEs are known to confer a fitness cost to their bacterial host. ICEs are known to contain genes that encode other beneficial phenotypes such as nitrogen fixation, aromatic compound degradation, and phage defense systems, however, it is not clear whether ICE*Mh*Susceptible confers any traits to its host (69–72).

Identification of ICEs containing the macrolide resistance gene *estT* provides an explanation for the observed resistance to the 16-membered macrolides tilmicosin (TILM) and tildipirosin (TILD), however it fails to explain the observed resistance to gamithromycin (GAM) and/or tulathromycin (TULA) in isolates containing ICE*MhI*-like01 since the *estT*-encoded esterase enzyme had no activity on gamithromycin (GAM) or tulathromycin (TULA) in a previous report (14). While the L23 ribosomal protein variant we identified partially explains the observed resistance to GAM in the isolates with the GAM/TULA/TET/TILM/TILD phenotype, we still lack an explanation for the observed GAM and TULA resistance in isolates with the TULA/TET/TILM/TILD and GAM/TULA/TILM phenotypes. Further investigation of the 79

candidate resistance genes identified in the multifactorial GLM analysis may offer such an explanation.

Conclusions

Our results reinforce the strong association of ICEs with AMR in *M. haemolytica*, with 90% of the resistant isolates examined in this study containing a putative ICE. The presence of *estT* explains the observed phenotypic resistance to the 16-membered lactone ring macrolides TILM and TILD, however based on previous reports of biochemical activity, it fails to provide an explanation for the observed resistance to GAM and/or TULA, in isolates with resistance to all four macrolides or those that exhibited resistance to TULA, TILM and TILD. In the isolates that are only resistant to GAM and TULA, the presence of *msr*(E) and *mph*(E) explained this observed phenotypic resistance. By quantifying the relationships between the presence/absence profiles of genes in the *M. haemolytica* pangenome and antimicrobial resistance phenotypes, we identified candidate genes that may contribute to the observed resistance and that should be studied further. We were also able to identify a GAM resistance-associated insertion in the L23 ribosomal protein gene and a macrolide resistance associated variant in the L22 ribosomal protein, however neither of these associations has been functionally verified. Finally, we found that ICEs containing no identifiable ARGs are common among susceptible isolates, which suggests that these elements may confer other fitness benefits to *M. haemolytica*. Taken together these results highlight that the success of diagnostic sequencing for detecting macrolide resistance will rely not only on the detection of well-established ARGs but also ongoing monitoring for novel mutations in the cellular targets of these antibiotics.

Data Availability

Assembled genome sequences have been deposited to NCBI under the BioProject accession PRJNA1088094.

Acknowledgements

The authors are grateful to Stacey Lacoste for assistance with the culture collection, to Haley Sanderson, Scott Dos Santos, and Dhinesh Periyasami for helpful discussions on the bioinformatic analysis, and to Dr. David Palmer (Dept. of Chemistry, University of Saskatchewan) for assistance with the protein structure alignment. Dr. Musangu Ngeleka (Prairie Diagnostic Services, Inc.) provided helpful feedback on the manuscript. This research was supported by grants from the Agriculture Development Fund and the Saskatchewan Cattlemen's Association.

References

1. DeDonder KD, Apley MD. 2015. A literature review of antimicrobial resistance in pathogens associated with bovine respiratory disease. *Anim Health Res Rev* 16:125–134.
2. Horton LM, Depenbusch BE, Dewsbury DM, McAtee TB, Betts NB, Renter DG. 2023. Comprehensive Outcomes Affected by Antimicrobial Metaphylaxis of Feedlot Calves at Medium-Risk for Bovine Respiratory Disease from a Randomized Controlled Trial. *Vet Sci* 10:67.
3. O'Connor AM, Hu D, Totton SC, Scott N, Winder CB, Wang B, Wang C, Glanville J, Wood H, White B, Larson R, Waldner C, Sargeant JM. 2019. A systematic review and network

548 meta-analysis of injectable antibiotic options for the control of bovine respiratory disease in
549 the first 45 days post arrival at the feedlot. *Anim Health Res Rev* 20:163–181.

550 4. Andrés-Lasheras S, Jelinski M, Zaheer R, McAllister TA. 2022. Bovine Respiratory
551 Disease: Conventional to Culture-Independent Approaches to Studying Antimicrobial
552 Resistance in North America. *Antibiotics* 11:487.

553 5. Alexander TW, Yanke LJ, Topp E, Olson ME, Read RR, Morck DW, McAllister TA. 2008.
554 Effect of Subtherapeutic Administration of Antibiotics on the Prevalence of Antibiotic-
555 Resistant *Escherichia coli* Bacteria in Feedlot Cattle. *Appl Environ Microbiol* 74:4405–
556 4416.

557 6. Government of Canada. 2017. Responsible use of Medically Important Antimicrobials in
558 Animals. [https://www.canada.ca/en/public-health/services/antibiotic-antimicrobial-](https://www.canada.ca/en/public-health/services/antibiotic-antimicrobial-resistance/animals/actions/responsible-use-antimicrobials.html)
559 [resistance/animals/actions/responsible-use-antimicrobials.html](https://www.canada.ca/en/public-health/services/antibiotic-antimicrobial-resistance/animals/actions/responsible-use-antimicrobials.html).

560 7. European Union. 2018. Regulation (EU) 2019/4 of the European Parliament and of the
561 Council on the manufacture, placing on the market and use of medicated feed, amending
562 Regulation (EC) No. 183/2005 of the European Parliament and of the Council and repealing
563 Council Directive 90/167/EEC.

564 8. European Union. 2018. Regulation (EU) 2019/6 of the European Parliament and of the
565 Council of 11 December 2018 on veterinary medicinal products and repealing Directive
566 2001/82/EC.

- 567 9. Hilt EE, Ferrieri P. 2022. Next Generation and Other Sequencing Technologies in
568 Diagnostic Microbiology and Infectious Diseases. *Genes* 13:1566.
- 569 10. Highlander SK. 2001. Molecular genetic analysis of virulence in *Mannheimia (Pasteurella)*
570 *haemolytica*. 3. *Front Biosci-Landmark* 6:1128–1150.
- 571 11. Brault SA, Hannon SJ, Gow SP, Warr BN, Withell J, Song J, Williams CM, Otto SJG,
572 Booker CW, Morley PS. 2019. Antimicrobial Use on 36 Beef Feedlots in Western Canada:
573 2008–2012. *Front Vet Sci* 6:329.
- 574 12. Snyder E, Credille B. 2020. *Mannheimia haemolytica* and *Pasteurella multocida* in bovine
575 respiratory disease: How are they changing in response to efforts to control them? *Vet Clin*
576 *North Am Food Anim Pract* 36:253–268.
- 577 13. Lubbers BV, Hanzlicek GA. 2013. Antimicrobial multidrug resistance and coresistance
578 patterns of *Mannheimia haemolytica* isolated from bovine respiratory disease cases—a
579 three-year (2009–2011) retrospective analysis: *J Vet Diagn Invest* 25:413–417.
- 580 14. Dhindwal P, Thompson C, Kos D, Planedin K, Jain R, Jelinski M, Ruzzini A. 2023. A
581 neglected and emerging antimicrobial resistance gene encodes for a serine-dependent
582 macrolide esterase. *Proc Natl Acad Sci* 120:e2219827120.
- 583 15. Rice JA, Carrasco-Medina L, Hodgins DC, Shewen PE. 2007. *Mannheimia haemolytica*
584 and bovine respiratory disease. *Anim Health Res Rev* 8:117–128.

- 585 16. Desmolaize B, Rose S, Warrass R, Douthwaite S. 2011. A novel Erm
586 monomethyltransferase in antibiotic-resistant isolates of *Mannheimia haemolytica* and
587 *Pasteurella multocida*. Mol Microbiol 80:184–194.
- 588 17. Michael GB, Kadlec K, Sweeney MT, Brzuszkiewicz E, Liesegang H, Daniel R, Murray
589 RW, Watts JL, Schwarz S. 2012. ICE*Pmul*, an integrative conjugative element (ICE) of
590 *Pasteurella multocida*: structure and transfer. J Antimicrob Chemother 67:91–100.
- 591 18. Eidam C, Poehlein A, Leimbach A, Michael GB, Kadlec K, Liesegang H, Daniel R,
592 Sweeney MT, Murray RW, Watts JL, Schwarz S. 2015. Analysis and comparative genomics
593 of ICE*Mhl*, a novel integrative and conjugative element (ICE) of *Mannheimia haemolytica*.
594 J Antimicrob Chemother 70:93–97.
- 595 19. Olsen AS, Warrass R, Douthwaite S. 2015. Macrolide resistance conferred by rRNA
596 mutations in field isolates of *Mannheimia haemolytica* and *Pasteurella multocida*. J
597 Antimicrob Chemother 70:420–423.
- 598 20. Younes JA, Ramsay DE, Lacoste S, Deschner D, Hill JE, Campbell J, Waldner CL. 2022.
599 Changes in the phenotypic susceptibility of *Mannheimia haemolytica* isolates to macrolide
600 antimicrobials during the early feeding period following metaphylactic tulathromycin use in
601 western Canadian feedlot calves. Can Vet J 63:920–928.
- 602 21. CLSI. 2020. VET01: Performance Standards for Antimicrobial Disk and Dilution
603 Susceptibility Tests for Bacteria Isolated From Animals, Fifth Edition. Wayne,
604 Pennsylvania, USA.

- 605 22. Martin-Platero AM, Valdivia E, Maqueda M, Martinez-Bueno M. 2007. Fast, convenient,
606 and economical method for isolating genomic DNA from lactic acid bacteria using a
607 modification of the protein “salting-out” procedure. *Anal Biochem* 366:102–4.
- 608 23. Links MG, Dumonceaux TJ, Hemmingsen SM, Hill JE. 2012. The chaperonin-60 universal
609 target is a barcode for bacteria that enables *de novo* assembly of metagenomic sequence
610 data. *PLoS ONE* 7:e49755.
- 611 24. Vancuren SJ, Hill JE. 2019. Update on cpnDB: a reference database of chaperonin
612 sequences. *Database* 2019:doi:10.1093/database/baz033.
- 613 25. Bolger AM, Lohse M, Usadel B. 2014. Trimmomatic: a flexible trimmer for Illumina
614 sequence data. *Bioinformatics* 30:2114–20.
- 615 26. Wick RR, Judd LM, Gorrie CL, Holt KE. 2017. Unicycler: Resolving bacterial genome
616 assemblies from short and long sequencing reads. *PLOS Comput Biol* 13:e1005595.
- 617 27. Shen W, Le S, Li Y, Hu F. 2016. SeqKit: A Cross-Platform and Ultrafast Toolkit for
618 FASTA/Q File Manipulation. *PLOS ONE* 11:e0163962.
- 619 28. Seemann T. 2014. Prokka: rapid prokaryotic genome annotation. *Bioinformatics* 30:2068–
620 2069.
- 621 29. Alcock BP, Raphenya AR, Lau TTY, Tsang KK, Bouchard M, Edalatmand A, Huynh W,
622 Nguyen A-LV, Cheng AA, Liu S, Min SY, Miroshnichenko A, Tran H-K, Werfalli RE, Nasir
623 JA, Oloni M, Speicher DJ, Florescu A, Singh B, Faltyn M, Hernandez-Koutoucheva A,
624 Sharma AN, Bordeleau E, Pawlowski AC, Zubyk HL, Dooley D, Griffiths E, Maguire F,

625 Winsor GL, Beiko RG, Brinkman FSL, Hsiao WWL, Domselaar GV, McArthur AG. 2020.
626 CARD 2020: antibiotic resistome surveillance with the comprehensive antibiotic resistance
627 database. *Nucleic Acids Res* 48:D517–D525.

628 30. Alcock BP, Huynh W, Chalil R, Smith KW, Raphenya AR, Wlodarski MA, Edalatmand A,
629 Petkau A, Syed SA, Tsang KK, Baker SJC, Dave M, McCarthy MC, Mukiri KM, Nasir JA,
630 Golbon B, Imtiaz H, Jiang X, Kaur K, Kwong M, Liang ZC, Niu KC, Shan P, Yang JYJ,
631 Gray KL, Hoad GR, Jia B, Bhando T, Carfrae LA, Farha MA, French S, Gordzevich R,
632 Rachwalski K, Tu MM, Bordeleau E, Dooley D, Griffiths E, Zubyk HL, Brown ED,
633 Maguire F, Beiko RG, Hsiao WWL, Brinkman FSL, Van Domselaar G, McArthur AG.
634 2023. CARD 2023: expanded curation, support for machine learning, and resistome
635 prediction at the Comprehensive Antibiotic Resistance Database. *Nucleic Acids Res*
636 51:D690–D699.

637 31. Seemann T. 2018. barnap 0.9: rapid ribosomal RNA prediction.

638 32. Seemann T. 2015. snippy: fast bacterial variant calling from NGS reads.

639 33. Page AJ, Cummins CA, Hunt M, Wong VK, Reuter S, Holden MTG, Fookes M, Falush D,
640 Keane JA, Parkhill J. 2015. Roary: rapid large-scale prokaryote pan genome analysis.
641 *Bioinformatics* 31:3691–3693.

642 34. Price MN, Dehal PS, Arkin AP. 2009. FastTree: Computing Large Minimum Evolution
643 Trees with Profiles instead of a Distance Matrix. *Mol Biol Evol* 26:1641–1650.

- 644 35. Walker BJ, Abeel T, Shea T, Priest M, Abouelliel A, Sakthikumar S, Cuomo CA, Zeng Q,
645 Wortman J, Young SK, Earl AM. 2014. Pilon: An Integrated Tool for Comprehensive
646 Microbial Variant Detection and Genome Assembly Improvement. *PLOS ONE* 9:e112963.
- 647 36. Masonbrink R. 2021. Multiple rounds of Pilon polishing/gap-filling on a genome assembly.
648 *Bioinforma Workb.*
649 [https://bioinformaticsworkbook.org/dataAnalysis/GenomeAssembly/Iterate_Pilon_Genome](https://bioinformaticsworkbook.org/dataAnalysis/GenomeAssembly/Iterate_Pilon_Genome_Polishing.html)
650 [_Polishing.html](https://bioinformaticsworkbook.org/dataAnalysis/GenomeAssembly/Iterate_Pilon_Genome_Polishing.html). Retrieved 6 September 2023.
- 651 37. Zhang Y, Park C, Bennett C, Thornton M, Kim D. 2021. Rapid and accurate alignment of
652 nucleotide conversion sequencing reads with HISAT-3N. *Genome Res* 31:1290–1295.
- 653 38. Danecek P, Bonfield JK, Liddle J, Marshall J, Ohan V, Pollard MO, Whitwham A, Keane T,
654 McCarthy SA, Davies RM, Li H. 2021. Twelve years of SAMtools and BCFtools.
655 *GigaScience* 10:giab008.
- 656 39. Lees JA, Galardini M, Bentley SD, Weiser JN, Corander J. 2018. pyseer: a comprehensive
657 tool for microbial pangenome-wide association studies. *Bioinformatics* 34:4310–4312.
- 658 40. Lees JA, Mai TT, Galardini M, Wheeler NE, Corander J. 2019. Improved inference and
659 prediction of bacterial genotype-phenotype associations using pangenome-spanning
660 regressions. *bioRxiv* <https://doi.org/10.1101/852426>.
- 661 41. R Core Team. 2021. R: A Language and Environment for Statistical Computing. Vienna,
662 Austria.

- 663 42. Clawson ML, Murray RW, Sweeney MT, Apley MD, DeDonder KD, Capik SF, Larson RL,
664 Lubbers BV, White BJ, Kalbfleisch TS, Schuller G, Dickey AM, Harhay GP, Heaton MP,
665 Chitko-McKown CG, Brichta-Harhay DM, Bono JL, Smith TPL. 2016. Genomic signatures
666 of *Mannheimia haemolytica* that associate with the lungs of cattle with respiratory disease,
667 an integrative conjugative element, and antibiotic resistance genes. BMC Genomics 17:982.
- 668 43. Buchan DWA, Jones DT. 2019. The PSIPRED Protein Analysis Workbench: 20 years on.
669 Nucleic Acids Res 47:W402–W407.
- 670 44. Liu M, Li X, Xie Y, Bi D, Sun J, Li J, Tai C, Deng Z, Ou H-Y. 2019. ICEberg 2.0: an
671 updated database of bacterial integrative and conjugative elements. Nucleic Acids Res
672 47:D660–D665.
- 673 45. Klima CL, Zaheer R, Cook SR, Booker CW, Hendrick S, Alexander TW, McAllister TA.
674 2014. Pathogens of Bovine Respiratory Disease in North American Feedlots Conferring
675 Multidrug Resistance via Integrative Conjugative Elements. J Clin Microbiol 52:438–448.
- 676 46. Altschul SF, Gish W, Miller W, Myers EW, Lipman DJ. 1990. Basic local alignment search
677 tool. J Mol Biol 215:403–410.
- 678 47. Desmolaize B, Rose S, Wilhelm C, Warrass R, Douthwaite S. 2011. Combinations of
679 macrolide resistance determinants in field isolates of *Mannheimia haemolytica* and
680 *Pasteurella multocida*. Antimicrob Agents Chemother 55:4128–4133.

48. Su W, Kumar V, Ding Y, Ero R, Serra A, Lee BST, Wong ASW, Shi J, Sze SK, Yang L, Gao Y-G. 2018. Ribosome protection by antibiotic resistance ATP-binding cassette protein. *Proc Natl Acad Sci* 115:5157–5162.
49. Conrad CC, Daher RK, Stanford K, Amoako KK, Boissinot M, Bergeron MG, Alexander T, Cook S, Ralston B, Zaheer R, Niu YD, McAllister T. 2020. A sensitive and accurate recombinase polymerase amplification assay for detection of the primary bacterial pathogens causing bovine respiratory disease. *Front Vet Sci* 7:208.
50. Stanford K, Zaheer R, Klima C, McAllister T, Peters D, Niu YD, Ralston B. 2020. Antimicrobial Resistance in Members of the Bacterial Bovine Respiratory Disease Complex Isolated from Lung Tissue of Cattle Mortalities Managed with or without the Use of Antimicrobials. 2. *Microorganisms* 8:288.
51. Wang Y, Niemi J, Airas K, Ylihonko K, Hakala J, Mäntsälä P. 2000. Modifications of aclacinomycin T by aclacinomycin methyl esterase (RdmC) and aclacinomycin-10-hydroxylase (RdmB) from *Streptomyces purpurascens*. *Biochim Biophys Acta BBA - Protein Struct Mol Enzymol* 1480:191–200.
52. Zaman S, Fitzpatrick M, Lindahl L, Zengel J. 2007. Novel mutations in ribosomal proteins L4 and L22 that confer erythromycin resistance in *Escherichia coli*. *Mol Microbiol* 66:1039–1050.
53. Nowakowski M, Inskeep P, Risk J, Skogerboe T, Benchaoui H, Meinert T, Sherington J, Sunderland S. 2004. Pharmacokinetics and lung tissue concentrations of tulathromycin, a new triamilide antibiotic, in cattle. *Vet Ther* 5:60–74.

- 702 54. Sauer RT, Baker TA. 2011. AAA+ Proteases: ATP-Fueled Machines of Protein Destruction.
703 Annu Rev Biochem 80:587–612.
- 704 55. Acharya S, Foster PL, Brooks P, Fishel R. 2003. The Coordinated Functions of the *E. coli*
705 MutS and MutL Proteins in Mismatch Repair. Mol Cell 12:233–246.
- 706 56. Sancar A, Williams KR, Chase JW, Rupp WD. 1981. Sequences of the *ssb* gene and protein.
707 Proc Natl Acad Sci 78:4274–4278.
- 708 57. Kramer G, Rauch T, Rist W, Vorderwülbecke S, Patzelt H, Schulze-Specking A, Ban N,
709 Deuerling E, Bukau B. 2002. L23 protein functions as a chaperone docking site on the
710 ribosome. Nature 419:171–174.
- 711 58. Allali N, Afif H, Couturier M, Van Melderen L. 2002. The Highly Conserved TldD and
712 TldE Proteins of *Escherichia coli* Are Involved in Microcin B17 Processing and in CcdA
713 Degradation. J Bacteriol 184:3224–3231.
- 714 59. Kaur G, Subramanian S. 2016. Classification of the treble clef zinc finger: noteworthy
715 lessons for structure and function evolution. Sci Rep 6:32070.
- 716 60. Donahue JL, Bownas JL, Niehaus WG, Larson TJ. 2000. Purification and Characterization
717 of *glpX*-Encoded Fructose 1,6-Bisphosphatase, a New Enzyme of the Glycerol 3-Phosphate
718 Regulon of *Escherichia coli*. J Bacteriol 182:5624–5627.
- 719 61. Cabedo H, Macián F, Villarroja M, Escudero JC, Martínez-Vicente M, Knecht E,
720 Armengod ME. 1999. The *Escherichia coli trmE (mnmE)* gene, involved in tRNA

721 modification, codes for an evolutionarily conserved GTPase with unusual biochemical
722 properties. EMBO J 18:7063–7076.

723 62. Mahdi AA, Sharples GJ, Mandal TN, Lloyd RG. 1996. Holliday Junction Resolvases
724 Encoded by Homologous *rusA* Genes in *Escherichia coli* K-12 and Phage 82. J Mol Biol
725 257:561–573.

726 63. González-Pastor JE, Hobbs EC, Losick R. 2003. Cannibalism by Sporulating Bacteria.
727 Science 301:510–513.

728 64. Vázquez-Laslop N, Mankin AS. 2018. How Macrolide Antibiotics Work. Trends Biochem
729 Sci 43:668–684.

730 65. Öhman A, Rak A, Dontsova M, Garber MB, Härd T. 2003. NMR structure of the ribosomal
731 protein L23 from *Thermus thermophilus*. J Biomol NMR 26:131–137.

732 66. Beker M, Rose S, Lykkebo CA, Douthwaite S. 2018. Integrative and Conjugative Elements
733 (ICEs) in Pasteurellaceae Species and Their Detection by Multiplex PCR. Front Microbiol
734 9:1329.

735 67. Cameron A, Zaheer R, McAllister TA. 2019. Emerging Variants of the Integrative and
736 Conjugant Element ICEMh1 in Livestock Pathogens: Structural Insights, Potential Host
737 Range, and Implications for Bacterial Fitness and Antimicrobial Therapy. Front Microbiol
738 10:2608.

739 68. Johnson CM, Grossman AD. 2015. Integrative and Conjugative Elements (ICEs): What
740 They Do and How They Work. Annu Rev Genet 49:577–601.

741 69. Wang M, Liu G, Liu M, Tai C, Deng Z, Song J, Ou H-Y. 2024. ICEberg 3.0: functional
742 categorization and analysis of the integrative and conjugative elements in bacteria. *Nucleic*
743 *Acids Res* 52:D732–D737.

744 70. Hirose J. 2023. Diversity and Evolution of Integrative and Conjugative Elements Involved
745 in Bacterial Aromatic Compound Degradation and Their Utility in Environmental
746 Remediation. *Microorganisms* 11:438.

747 71. Johnson CM, Harden MM, Grossman AD. 2022. Interactions between mobile genetic
748 elements: An anti-phage gene in an integrative and conjugative element protects host cells
749 from predation by a temperate bacteriophage. *PLoS Genet* 18:e1010065.

750 72. Haskett TL, Ramsay JP, Bekuma AA, Sullivan JT, O’Hara GW, Terpolilli JJ. 2017.
751 Evolutionary persistence of tripartite integrative and conjugative elements. *Plasmid* 92:30–
752 36.

753

754

755

Table 1. Antibiotic resistance phenotypes of study isolates

Phenotype ¹	Number of Isolates
Susceptible	47
GAM/TULA/TET/TILM/TILD	27
TULA/TET/TILM/TILD	11
GAM/TULA	8
TET/TILM/TILD	5
GAM/TULA/TILM	1
Total	99

756

757

758

759

¹GAM = gamithromycin, TULA = tulathromycin, TILM = tilmicosin, TILD = tildipirosin, TET = tetracycline. GAM, TULA, TILM and TILD are all macrolide class antibiotics. TET is a tetracycline class antibiotic.

760

761

762

763

764

Phenotype ¹	No. of isolates	<i>msr</i> (E)	<i>mph</i> (E)	<i>erm42</i>	<i>sul2</i>	<i>tet</i> (H)	APH(3'')-1b	APH(3')-1a	APH(6)-1d	<i>estT</i>
GAM/TULA	8	8/8	8/8	0/8	7/8	0/8	0/8	0/8	0/8	0/8
GAM/TULA/TET/TILM/TILD	27	0/27	0/27	0/27	25/27	27/27	27/27	27/27	27/27	27/27
TULA/TET/TILM/TILD	11	0/11	0/11	0/11	11/11	11/11	11/11	11/11	11/11	11/11
TET/TILM/TILD	5	0/5	0/5	0/5	5/5	5/5	5/5	5/5	5/5	5/5
GAM/TULA/TILM	1	0/1	0/1	0/1	1/1	1/1	1/1	1/1	1/1	1/1
Susceptible	47	0/47	0/47	0/47	0/47	0/47	0/47	0/47	0/47	0/47

Table 2. Antibiotic resistance genes detected in study isolates.

¹GAM = gamithromycin, TULA = tulathromycin, TET = tetracycline, TILM = tilmicosin, TILD = tildipirosin.

Table 3. Results of unifactorial and multifactorial GLMs for each antibiotic. Shown are the p-values for the three explanatory factors: genotype, *tet*(H), and *msr*(E).

Analysis	Drug	genotype	<i>tet</i>(H)	<i>msr</i>(E)
Unifactorial	GAM	0.33	4.9e-07	3.2e-05
Unifactorial	TULA	0.97	1.67e-14	0.0004
Unifactorial	TET	2.6e-06	< 2.2e-16	0.002
Unifactorial	TILM	1.8e-06	< 2.2e-16	0.002
Unifactorial	TILD	2.6e-06	< 2.2e-16	0.002
Multifactorial	GAM	0.52	1.4e-10	1.2e-06
Multifactorial	TULA	0.52	< 2.2e-16	1.2e-06
Multifactorial	TET	0.52	< 2e-16	> 0.99
Multifactorial	TILM	0.52	< 2e-16	> 0.99
Multifactorial	TILD	0.52	< 2e-16	> 0.99

770 **Table 4.** Distribution of identified putative ICEs in *M. haemolytica* isolates in the present study.

Phenotype	No. of isolates	ICEM <i>hI</i> -like01	ICEM <i>h</i> GAMTULA	ICEM <i>h</i> Susceptible
Susceptible	47	0	0	19
GAM/TULA/TET/TILM/TILD	27	24	0	0
TULA/TET/TILM/TILD	11	10	0	0
TET/TILM/TILD	5	5	0	0
GAM/TULA	8	0	7	0
GAM/TULA/TILM	1	1	0	0
Direct Repeat Sequence		cgtgtcgggtcgagtcgacc	aaataataatgaaaa	cgtgtcgggtcgagtcgacc
Total	99	40	7	19

771

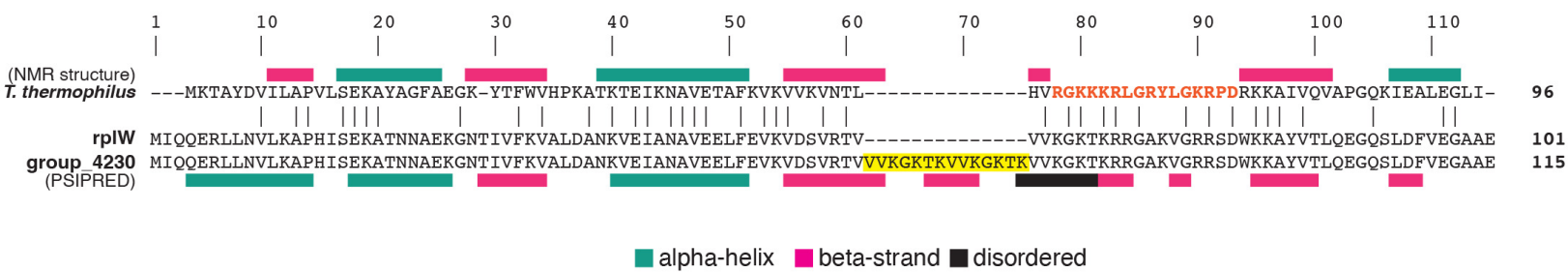
772

Figure Captions

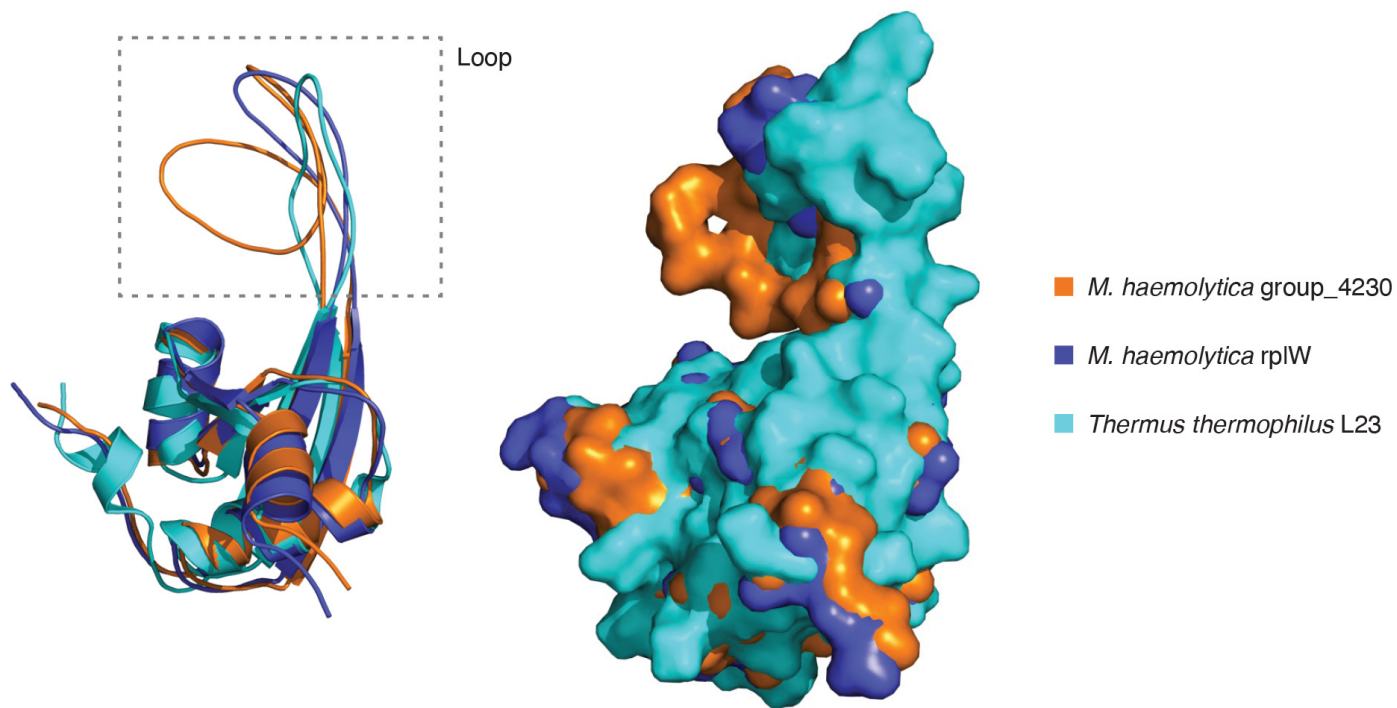
Figure 1. (A) Alignment of the amino acid sequences of L23 ribosomal proteins from *T. thermophilus* (PDB accession 1N88) and *M. haemolytica* (rplW and group_4230). A 14-amino acid insertion in group_4230 is indicated by yellow highlighting, and the flexible loop of L23 by orange text. Secondary structure features (determined by NMR for *T. thermophilus* or predicted by PSIPRED and DISOPRED3 for *M. haemolytica* sequences) are indicated above and below the alignment according to the legend. Sequences were aligned using MUSCLE pairwise alignment in Geneious Prime with default settings. (B) Ribbon (left) and space-filling models (right) of the alignment of the NMR structure of *T. thermophilus* L23 with predicted structures of *M. haemolytica* rplW and group_4230. The loop structure that is extended by the insertion in group_4230 is indicated on the ribbon diagram.

Figure 2. Putative ICE sequences identified in *M. haemolytica* isolates in the present study, ICEMhI-like01, ICEMhGAMTULA and ICEMhSusceptible. ICEMhI (top) is included for reference. Regions containing known ARGs are expanded to show detailed gene organization. ARGs, ICE-associated genes (encoding relaxases, transposases, integrases, and other functions) and genes encoding hypothetical proteins are indicated by colour according to the legend. Scale bar indicates 20 kilobase pairs.

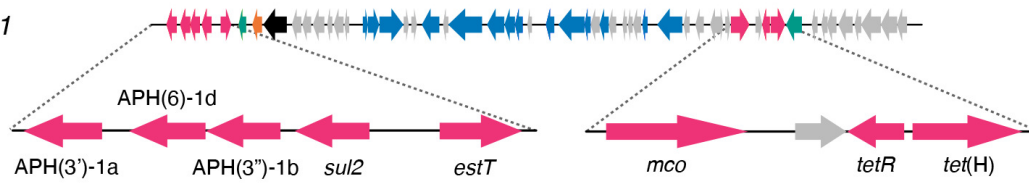
A.



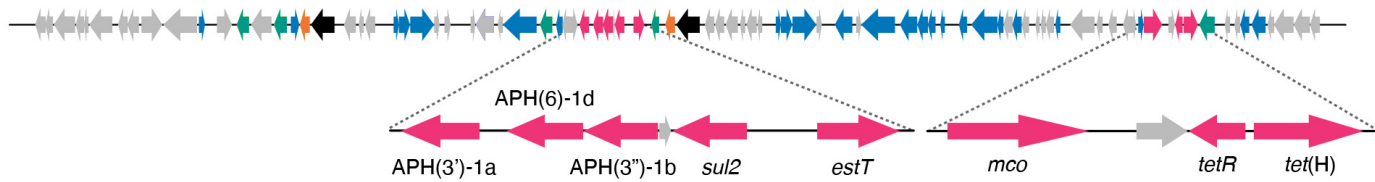
B.



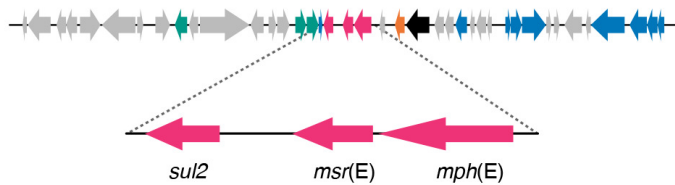
ICEMh1



ICEMh1-like01



ICEMhGAMTULA



ICEMhSusceptible



- AMR gene
- Relaxase
- Transposase
- Integrase
- Other ICE related function
- Hypothetical protein

20 kb